REPORT DOCUMENTATION PAGE

Form Approved
OMB No. 0704-0188

1. AGENCY USE ONLY (Leave Blank)	2. REPORT DATE	3. REPORT TYPE AND DATES COVERED
	31 October 1996	Professional Paper

4. TITLE AND SUBTITLE

Superconducting Gyroscope

5. FUNDING NUMBERS

6. AUTHOR(S)

Francis A. Karwacki, Martin A. Sanzari, and H. L. Cui

7. PERFORMING ORGANIZATION NAMES(S) AND ADDRESS(ES)

COMMANDER
NAVAL AIR WARFARE CENTER AIRCRAFT DIVISION
22541 MILLSTONE ROAD
PATUXENT RIVER, MD 20670-5304

8. PERFORMING ORGANIZATION REPORT NUMBER

9. SPONSORING / MONITORING AGENCY NAME(S) AND ADDRESS(ES)

Office of Naval Research (331)
800 Quincy Street
Arlington, VA 22217-5660

10. SPONSORING / MONITORING AGENCY REPORT NUMBER

11. SUPPLEMENTARY NOTES

12a. DISTRIBUTION / AVAILABILITY STATEMENT

APPROVED FOR PUBLIC RELEASE: DISTRIBUTION UNLIMITED

12b. DISTRIBUTION CODE

13. ABSTRACT (Maximum 200 words)

A brief description of the theory of operation of superconducting Gyroscope (SG) will be presented. In addition, the theory of a unique magnetic shield design will be presented along with experimental data on the shielding factor and the London Field Experimental data will also be presented.

Subject Terms
SUPERCONDUCTING GYROSCOPE
SPLIT MAGNETIC SHIELD DESIGN
INERTIAL SENSOR APPLICATION

15. NUMBER OF PAGES
31

16. PRICE CODE

17. SECURITY CLASSIFICATION OF REPORT	18. SECURITY CLASSIFICATION OF THIS PAGE	19. SECURITY CLASSIFICATION OF ABSTRACT	20. LIMITATION OF ABSTRACT
UNCLASSIFIED	UNCLASSIFIED	UNCLASSIFIED	N/A

NSN 7540-01-280-5500

Standard Form 298 (Rev. 2-89)
Prescribed by ANSI Std. Z39-18
298-102

DISCLAIMER NOTICE

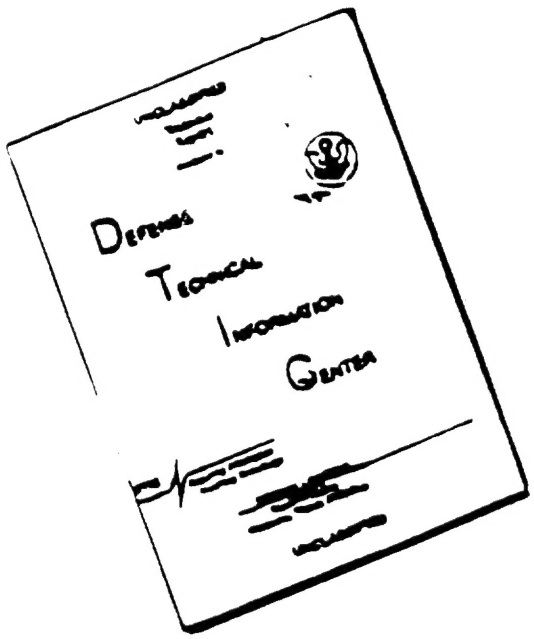

THIS DOCUMENT IS BEST QUALITY AVAILABLE. THE COPY FURNISHED TO DTIC CONTAINED A SIGNIFICANT NUMBER OF PAGES WHICH DO NOT REPRODUCE LEGIBLY.

Martin A.Sanzari
Department of Physics, Fordham University, Bronx, NY 10458

Francis A. Karwacki
Naval Air Warfare Center, AirCraft Division, Patuxent River, MD 20670-5304

H.L. Cui
Department of Physics, Stevens Institute of Technology, Hoboken, NJ 07030

Superconducting Gyroscope

A brief description of the theory of operation of the Superconducting Gyroscope (SG) will be presented. In addition, the theory of a unique split magnetic shield design will be presented along with experimental data on the shielding factor and the London Field. Experimental data will also be presented.

Introduction

The Superconducting Gyroscope (SG) is a new-concept gyro that is being investigated to determine its potential for inertial sensor applications. The SG utilizes Josephson junctions and the phase coherence of the superconducting electrons to measure rotation about a sensitive axis. Our design approach is to use a ring with two Josephson junctions (a Superconducting QUantum Interference Device (SQUID)) with a multilayered split superconducting shield, (Figure 1). As the superconducting electrons enter, a portion of them travel around the ring in the clockwise direction, an equal portion will travel around in the counter-clockwise direction. As they travel in their respective directions, the Cooper-paired electrons will experience an equal but opposite phase shift. This phase shift manifests itself by the use of the two Josephson junctions, one in each leg of the ring. As the paired electrons travel through their respective Josephson junctions, a shift occurs in the respective currents on the other side of the junction. As these two currents are combined at the bottom portion of the ring, a $\cos^2\phi$ pattern will be produced in the output voltage (Figure 2), where ϕ is the phase shift. The voltage that develops across the SQUID is given by

$$\Delta V_{SQUID}(B,\omega) = \frac{R}{2}\sqrt{I^2 - 4I_o^2\cos^2(\Delta\phi_\omega + \Delta\phi_B)} \qquad (1)$$

where $\Delta\phi_B = \pi\Phi / \Phi_o$, the change in phase resulting from magnetic field changes in the area enclosed by the SQUID. The change in phase resulting from rotation is given by: $\Delta\phi_\omega = 4m_e S\omega / \hbar$, where m_e is the free electron mass, ω is the applied rotation, and S is the area enclosed by the ring. The change in phase that results from rotation can be written as:

$$\Delta\phi_\omega = \pi\frac{\delta\omega\, S}{h/4m} = \pi\frac{\delta\Omega}{\Omega_o} \qquad (2)$$

where $\Omega_o = h / 4m$ is the quantum circulation. To measure rotation effectively, $\Delta\phi_B$ must

be equal to zero. This requires that the magnetic field changes in the area of the SQUID be held to zero. This can be accomplished by surrounding the SQUID with a superconducting shield. The SQUID's sensitivity to magnetic fields can be used to facilitate the design of a closed loop rotation sensing system. The argument of the cosine term in equation (1) can be held to zero by requiring that the phase change resulting from rotation be cancelled by a phase change equal in magnitude and opposite in direction. This can be accomplished by placing a feedback coil next to the SQUID (Figure 3). The feedback coil will generate a magnetic field at the precise intensity to cancel the action resulting from the rotation. Therefore, the voltage of the SQUID will be held at a constant value using a magnetic feedback coil as a phase rebalance (Figure 4). The current supplied to the feedback coil to maintain a constant voltage will be proportional to the applied rotational velocity.

Changes from external magnetic fields can be minimized by enclosing the SQUID in a superconducting shield. It is important to consider the effect of rotation if both the SQUID and the superconducting shield share the same rotation. Assume the SQUID is centered in a superconducting spherical shell and both are rotating with the same angular velocity (Figure 5). The spherical shell will generate a magnetic field (the London field) $B_L = -2\ mc\omega/e$, where $e < 0$, which appears as an externally applied field to the SQUID. Therefore the rotating spherical shell can be replaced with an equivalent external field which equals $B_{ext} = -2mc\omega/e$ (Figure 6). The rotating SQUID is generating a magnetic field also equal to B_L. This is a result of the electrons in the surface of the superconducting shell lagging behind the lattice. This surface current is denoted as I_L and has a net flow in the clockwise direction, assuming the angular velocity is counterclockwise (Figure 7). The SQUID will still act to expel external fields. The external field that was generated by the rotating spherical shell produced a magnetic field in the same direction and magnitude as the field generated by the rotating SQUID. A surface current is generated in the SQUID to expel the external field, this current will be equal in magnitude and opposite in direction as the London drag current in the SQUID (Figure 8). These two currents will cancel and there will

be no change in voltage across the SQUID. The superconducting shield that protects the SQUID from external fields causes the SQUID to be completely insensitive to rotation . To prevent the formation of the London field in the superconducting shield and still provide magnetic shielding, a hollow cylindrical shield with a small discontinuity down the length of the shield will be used (Figure 9). For a discontinuity greater than the coherence length, the superelectrons cannot cross the boundary and prohibit the formation of the London drag current necessary for the formation of the London field. This does not, however, adversely effect the ability of the cylindrical superconductor to act as a magnetic shield. Localized Eddy currents will form to prevent external magnetic fields from penetrating into the shield (Figure 10). It can be shown that any external magnetic field impinging directly on the discontinuity will be attenuated by many orders of magnitude. The shielding factor (SF) for a split-superconducting shield is defined as $B_\theta (R_1, \theta) / B_o$ cosine θ is given by:

$$SF(R_1, \theta) = \frac{B_\theta (R_1, \theta)}{B_o \cos\theta} = \frac{1}{2\pi\rho} \sum_{m=0}^{\infty} \ln \left| \frac{1 + \rho^{2(2m+1)} + 2\rho^{2m+1} \cos(\theta + \delta\theta)}{1 + \rho^{2(2m+1)} + 2\rho^{2m+1} \cos(\theta - \delta\theta)} \right| \qquad (3)$$

where R_1 is the radius of the shield and $2\delta\theta$ is the angle formed by the width of the slit. For a shield with a radius of $R_1 = 1 \times 10^{-2}$ m and $\delta\theta = 0.02$ radians, the estimated shielding factor is 0.5×10^{-10} on the inner wall 180 degrees from the opening $2\delta\theta$. This shielding factor can be increased by nesting cylindrical shields concentrically and alternating the slit openings 180 degrees from each other.

This paper presents important findings concerning the achievement in developing a SG. Information is presented on the manner in which detection of rotation is achieved using a SQUID, how external magnetic field attenuation is achieved on an experimental level to detect rotation (to the limit of the SQUID electronics), experimental results on the decoupling the London field produced by a rotating superconductor from eliminating the sensitivity of the SQUID to detect rotation, and measurements of rotation via SQUID detection of the London field from a rotating superconductor (first step in determining sensitivity and the ability of the SQUID to detect rotation).

Theory of Rotation Detection

A commercial dc SQUID was used to measure the magnetic field in the rotating superconductor and in experiments to directly measure rotation. The external flux, Φ_{ext} from the sample was coupled into the single turn Pickup Coil of inductance L_p. This induces a current, I, in the circuit which couples a flux Φ_{SQUID} into the SQUID through the Input Coil of inductance L (Figure 11)[i]. The mutual inductance of the Input Coil and the SQUID is shown as M_i. The equation which relates the external flux coupled into the circuit to the flux in the SQUID can be written using the property of conservation of flux in a superconducting circuit.

$$\Phi_{ext} = (L_p + L_i)\left(\frac{\Phi_{SQUID}}{M_i}\right) \tag{4}$$

Note, that for purposes of this paper, currents in the SQUID itself may be ignored. These are typically very high frequencies and have little effect on this analysis. Note that by substituting $\Phi_{SQUID,n}$, the SQUID flux noise, for Φ_{SQUID}, this equation yields external flux sensitivity, $\Phi_{ext,n}$, of the circuit. That is, the minimum flux coupled into the input coil to which the system is sensitive. This is the parameter which one typically wishes to optimize. Expressing the mutual inductance as

$$M_i = k\sqrt{L_i L_{SQUID}} \tag{5}$$

substituting into equation (4)

$$\Phi_{ext,\eta} = \frac{(L_p + L_i)}{k\sqrt{L_i L_{SQUID}}}\Phi_{SQUID,\eta} \tag{6}$$

Field sensitivity is often a better parameter to use instead of flux sensitivity, so re-expressing in terms of the external applied magnetic field,

$$B_{ext,\eta} = \frac{(L_p + L_i)}{A\,k\sqrt{L_i\,L_{SQUID}}}\,\Phi_{SQUID,\eta} \tag{7}$$

where $B_{ext,\eta}$ is the external field sensitivity and A is the area of the pickup coil. Note that we are assuming a uniform external field. It is easily determined that to optimize the sensitivity with respect to the input coil inductance L_i, we need to have $L_i = L_p$. That is, we need to match the inductances of the input and pickup coils. Under this condition, the sensitivity becomes,

$$\Phi_{ext,\eta} = \frac{2\,L_p}{k\sqrt{L_{SQUID}}}\,\Phi_{SQUID,\eta} \tag{8}$$

Examining equation (7), it would appear that smaller pickup coil inductances would be best since this would minimize $B_{ext,\eta}$. However, this is not necessarily the proper conclusion. Closer attention needs to be paid to the other two terms in the equation. For example, the area A and the inductance of the pickup coil are related. Typically, the area of a single turn loop is proportional to the square of the inductance so we can substitute CL_p^2 for A, where C is a constant of proportionality. This gives,

$$B_{ext,\eta} = \frac{(L_p + L_i)}{C\,L_p^2\,k\sqrt{L_i\,L_{SQUID}}}\,\Phi_{SQUID,\eta} \tag{9}$$

Examining this equation, it is seen that the larger the inductance of the pickup coil, the more sensitive the system appears to be. This is true, however, only for a uniform field such that the coupled flux increases in proportion to the square of the inductance (that is, in proportion to the area of the coil). Examining other field configurations such as from a point dipole source, we see the opposite result. The flux from a point dipole coupling into a circular coil is,

$$\Phi_m = \frac{\mu_o}{2}\frac{m}{r} \tag{10}$$

where μ_o is the permeability of free space, m is the dipole strength, and r is the radius of the coil. Substituting this into equation (6) and solving for m, we find the minimum detectable dipole strength is,

$$m_{ext,\eta} = \frac{2r(L_p + L_i)}{\mu_o k\sqrt{L_i L_{SQUID}}}\Phi_{SQUID,\eta} \tag{11}$$

Note that since the inductance L_p is proportional to r, it would appear that in this case smaller pickup coils would be optimum. Therefore, configuration of the pickup coils is primarily determined by considering how to most effectively couple to the magnetic field being measured. Once the pickup coil has been configured, the pickup coil-SQUID circuit can be optimized. One method of optimization is to vary the number of turns that make up the pickup coil. To optimize a multiloop circuit, equation (6) can be rewritten as

$$\Phi_{ext,\eta} = B_{ext,\eta} A = \frac{1}{n}\frac{(n^2 l_p + L_i)}{k\sqrt{L_i L_{SQUID}}}\Phi_{SQUID,\eta} \tag{12}$$

where n is the number of turns in the coil and $L_p = n^2 l_p$. Maximizing equation (12) with respect to n, we find that the optimum number of turns is,

$$n = \sqrt{\frac{L_i}{l_p}} \tag{13}$$

Using these relationships for maximizing the flux sensitivity of the SQUID, the following parameters will be used for the pickup coil in the London moment experiment: 16 turns

of 0.015 inch diameter niobium wire will be used to form a 0.460 inch diameter pickup coil.

Magnetic Shielding For Rotation Detection

The experimental setup used a multi-nested configuration of Nb and Pb to achieve the necessary attenuation of external fields below nanogauss levels. The shield configuration consisted of two Nb shield followed by two Pb shields closer to the site of the experimental set up (Figure 12). In order to determine the resolution of the SQUID detector in this shield configuration a measurement of the residual magnetic field as a function of time was performed. The changes in the magnetic field as a function of time in the work area were so low that the changes appeared as jumps from one level to the next level (Figure 13). To ascertain the origin of these jumps, the SQUID was disassembled and the screw connections for the pickup coil were shorted with a small piece of niobium wire. The SQUID was reassembled and the magnetic field was monitored. The same jumps appeared in this data (Figure 14). Since the SQUID was shorted, the jumps corresponded to the limit of the analog to digital (A/D) converter. These jumps corresponded to a voltage change $\Delta V_{SQUID} = 150\ \mu V$, using the scale factor for the SQUID system this corresponds to 0.00365 Φ_o, which is equal to 7.552×10^{-10} gauss cm^2. Therefore, the magnetic shielding was adequate enough to permit the measurement of magnetic field changes to the resolution of the A/D converter in the SQUID controller. In a short time scale, the A/D of the SQUID controller limits the resolution. In the long term, drift in the SQUID system is the main source of potential errors. The measured drift for the SQUID system is 0.0051 Φ_o /min = 1.072×10^{-9} gauss cm^2/min.

Measurement of Split Superconducting Shield London Field and Shielding Capabilities

Two superconducting shields were fabricated to examine the London field and shielding generated by localized Eddy currents in the penetration depth of the superconductor. The shields were grown by laser ablation of YBCO on $SrTiO_3$. The $SrTiO_3$ crystal samples were parallelepiped (Figure 15). They were mounted in a laser ablation chamber, heated to the proper temperature and coated with YBCO to a thickness of 2000 Å. After coating they where x-rayed to determine their composition and then sent to the laboratory for evaluation, the shield was mounted into the first rotational probe and rotated. The rotation was from 40 RPM clockwise to 40 RPM counterclockwise. The shift in the out voltage of the SQUID was 0.1 volt which corresponds to a London field of 7.8×10^{-8} Φ_o. The shield was then removed, one corner of the parallel-pipe head was scored to provide a break in the material wider than the coherence length (Figure 16)., The shield was than place back into the rotational probe and rotated. The SQUID output voltage did not show a shift in DC level for rotation rates from ±10 to ±100 rpm (Figure 17) . The SQUID did show an oscillation which indicated that the trapped flux was being pushed by the side walls of the shield (Figure 18). The localized currents were pushing the flux lines out of the superconducting material. It can therefore be said that the side wall can act as a shield to magnetic fields and that a multi-layered shield will provide the necessary shielding for the gyroscope.

In addition to the experimental data a revised analysis of the shielding factor of a split superconducting magnetic shield was performed as previously discussed. For a shield with a radius of $R_I = 1 \times 10^{-2}$ m and $\delta\theta = 0.02$ radians (Figure 18), the estimated shielding factor is 0.5×10^{-10} on the inner wall 180 degrees from the opening $2\delta\theta$. This shielding factor can be increased by nesting cylindrical shields concentrically and alternating the split openings 180 degrees from each other.

Measurement of Rotation Using London Field

The London field was measured by rotating a cylindrically shaped superconductor in a flux transformer in liquid helium. All the measurements were done by first cooling the work area and the test assembly to 4.2 K and then setting the sample into rotation. A Pb sample having the same dimensions as the HfV_2 and BiPbSrCaCuO samples is used to calibrate the measurement (Figure 19). The London field of lead has been measured by Hildebrandt on a Pb film and a lead foil, which produced a London field slope of $B = 1.09 \times 10^{-11}\ \omega$ Tesla with an accuracy of ± 7%. The theoretical value is $B = 1.137 \times 10^{-11}\ \omega$ Tesla with ω in rad/s. The change in the SQUID output voltage vs frequency of rotation was a linear relationship. The data taken for both samples shows this relationship. A least squares fit to the data points gives a slope of 0.009562 ± 0.0002 Vs/rad. During data collection the SQUID output voltage was filtered with a 1 Hz filter to remove an ac signal oscillating at the frequency of rotation. This was a result of a slight shaft wobble. This was separated out by rotating the shaft slowly by hand and using the recorded data during data processing. To compare this result to the theoretical value of the London field, corrections to equation (21) must be considered. The equation for the measured London field slope with corrections is given by:

$$\left(\frac{B}{\omega}\right)_{corrected} = \left(\frac{\Delta V_{SQUID}}{\Delta \omega} - \frac{\Delta V_{Holder}}{\Delta \omega}\right) \frac{(2\pi)(SF)\Upsilon}{S_{coil}} (2.0678\times10^{-15}) \qquad (23)$$

which yields a value of 1.075×10^{-7}, which is within 5% of the theoretical value. Therefore, the measurement of lead can be used as a calibration for the measurement on the HfV_2 and BiPbSrCaCuO superconductors. The London field slope of HfV_2 has the same value as the lead sample to within the experimental error. A least squares fit to the data points gives a London field slope of 0.09771 ± 0.0003 Vs/rad for HfV_2 as compared to 0.009562 ± 0.0002 Vs/rad for lead (Figure 20). For all the samples, the field reverses upon changing the direction of rotation. In order to make continuous measurements through zero, the motor

speed had to be reduced in a very smooth and extremely slow motion. Any jerking of the shaft would produce an offset as the measurement went through zero. It is extremely important that all motion has stopped in one direction before starting to rotate in the opposite direction. It is also clear that the sign of the London slope is the same for all three samples. The data clearly illustrated that the effective mass of the heavy fermion does not influence the sensitivity of the scale factor of the gyroscope.

In previous measurements of the London field , the slowest rates of rotation (20-1050 rpm) were measured by Brickman. The main problem with making a London field measurement at such slow rotation rates is the inability to maintain a test environment free from magnetic field changes. As previously pointed out, the magnetic field changes in the test system were extremely low. A London field measurement was performed in a frequency range of 0.6 - 7.8 rpm. The speed changes were not continuous, changes were made in jumps of ~1 rpm. This procedure permitted the differentiation between changes in the London field resulting from rotation and any drift from the SQUID system. The test was performed at night when the electromagnetic activity in the building was a minimum. At each speed the SQUID voltage jumped back and forth between its resolution limited (as a result of the A/D converter) values. If any changing magnetic fields in the test environment were contributing a drift to the measurement, this type of jumping back and forth between levels would have appeared as an array of continuous jumps in the upward or downward direction. A synchronous data collection program was used. Data was taken at the same point during each rotation. This procedure is most effective at slow rotation rates. This test provides a verification of the London field at low rotation rates , where no previous work has been reported. A least-squares fit to the data points gives a slope of 0.009260 ± 0.0008 Vs/rad, which is within experimental error (~3%) compared to lead. A demonstration of the ability to detect rotation at such slow rates is a demonstration of gyroscope application.

Conclusion

Several major accomplishments have been achieved over this past fiscal year which shows the potential of the SG. First, the external field has been attenuated to 7.552×10^{-10} gauss cm^2 allowing rotation measurements to within the current limit of the SQUID electronics. Second, the drift in the SQUID electronics is 1.072×10^{-9} gauss cm^2/min. This is with standard SQUID electronics and no external control to stablize temperature.. Third, the split superconducting gyro shield design shows no London field and uses surface eddy currents to expel external flux (theoretical SF=0.5×10^{-10}). Fourth, the London field has been measured to 0.025 rad/sec. This shows the potential of rotation measurement using superconductivity. The next step in the program is to rotate the SQUID within a split superconducting shield . This would have to be accomplished in conjunction with modification to the SQUID electronics to improve the detection capability and drift.

Acknowledgements

The authors of this paper would like to thank the Office of Naval Research and Special Projects-24 Office for their program support. In addition, we would like to thank Kearfott Guidance and Navigation Company and Temple University for cooperation in the development and evaluation of structures for the program.

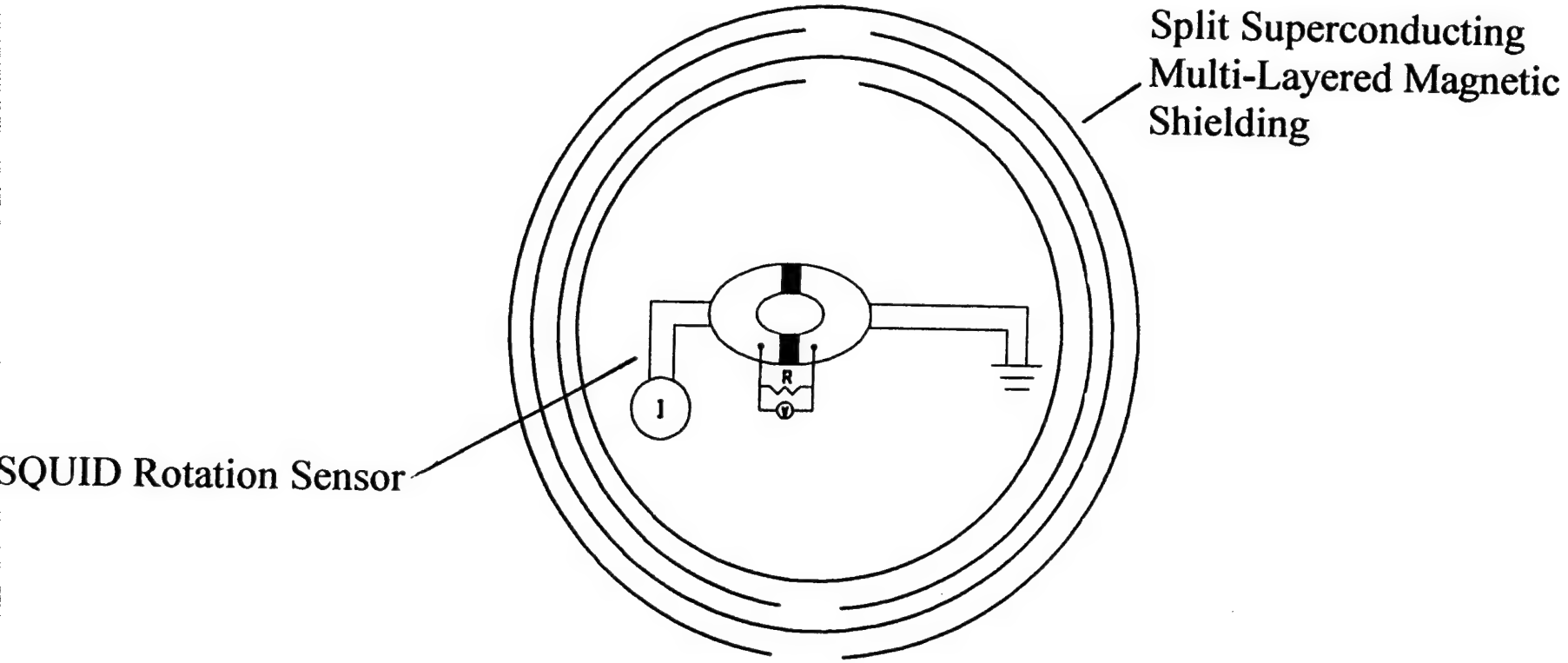

Figure 1 : Superconducting Gyroscope

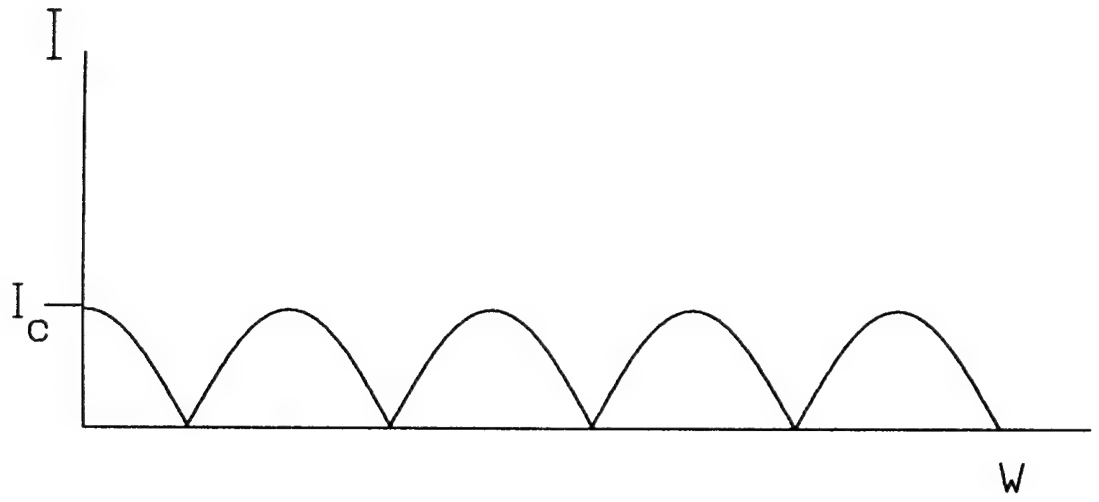

Figure 2 : SQUID Output Current

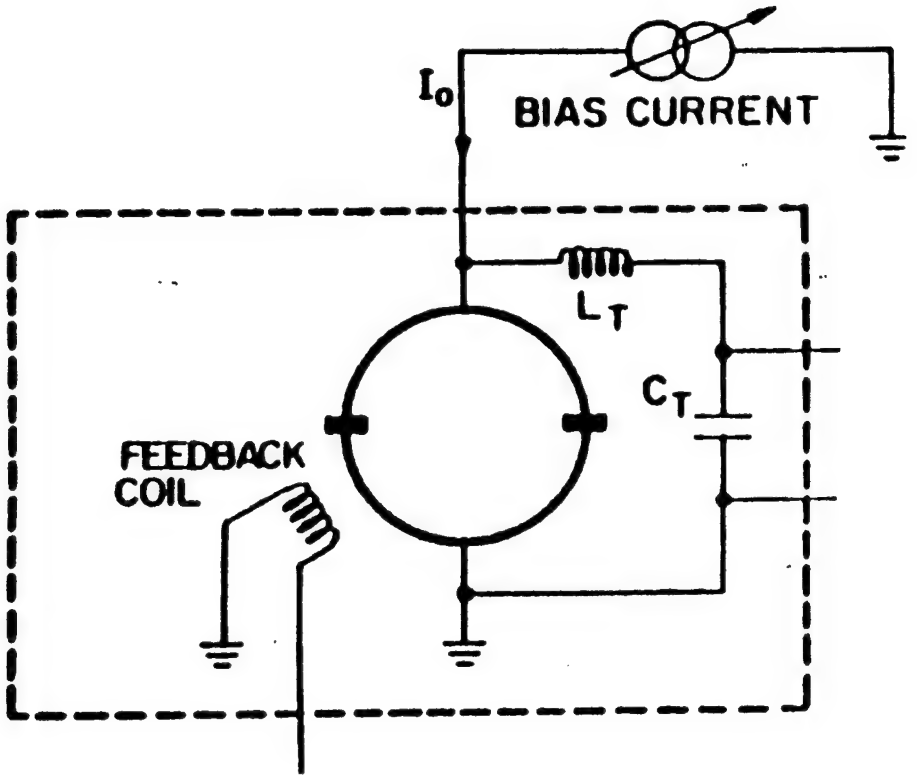

Figure 3 : SQUID with Feedback Coil

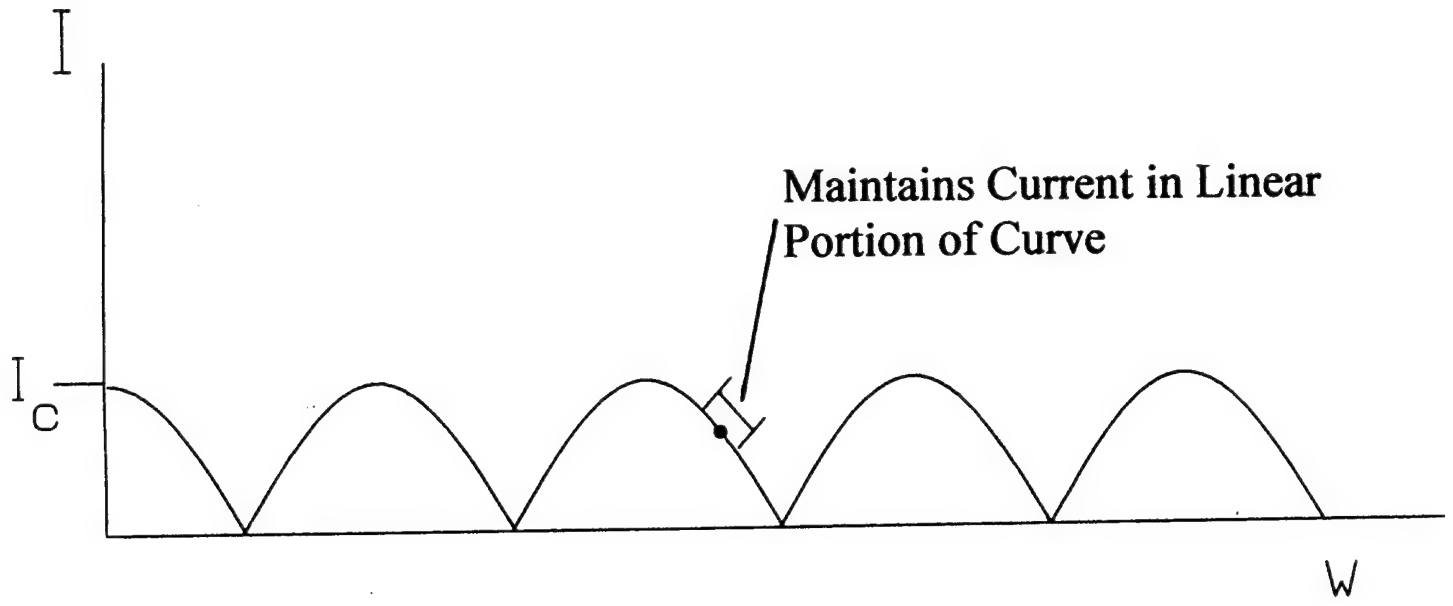

Figure 4 : SQUID Output Current with Feedback Control

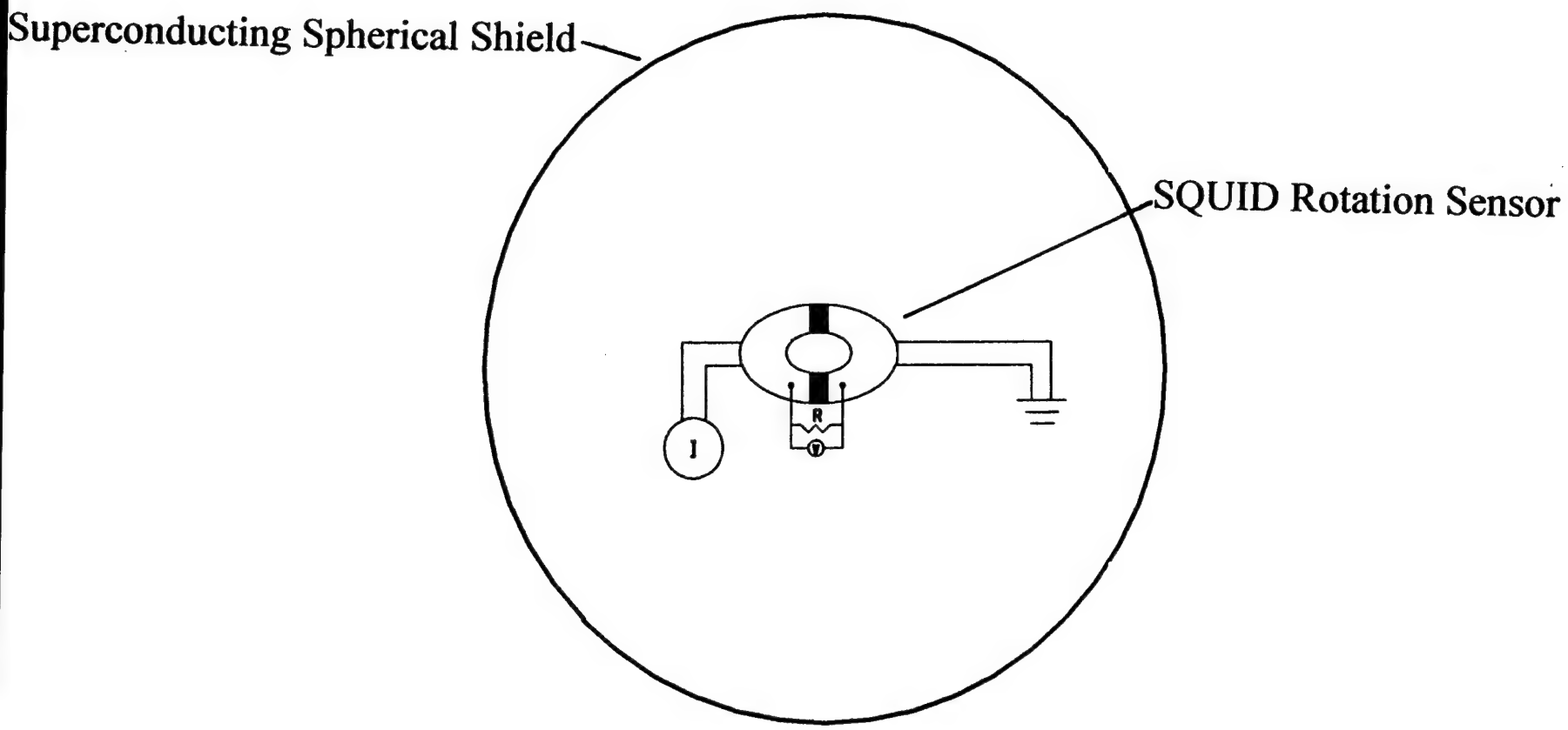

Figure 5 : Squid in Superconducting Spherical Shield

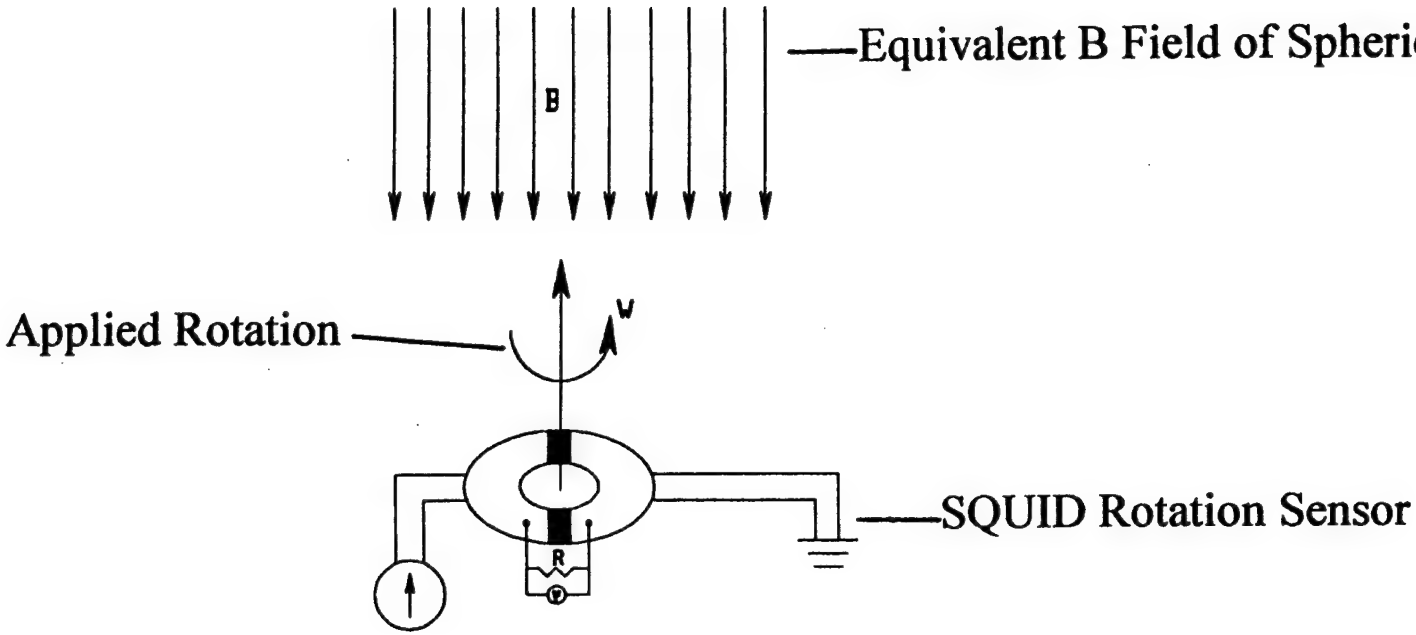

Figure 6 : Superconducting Spherical Shield Replaced by Constant B Field

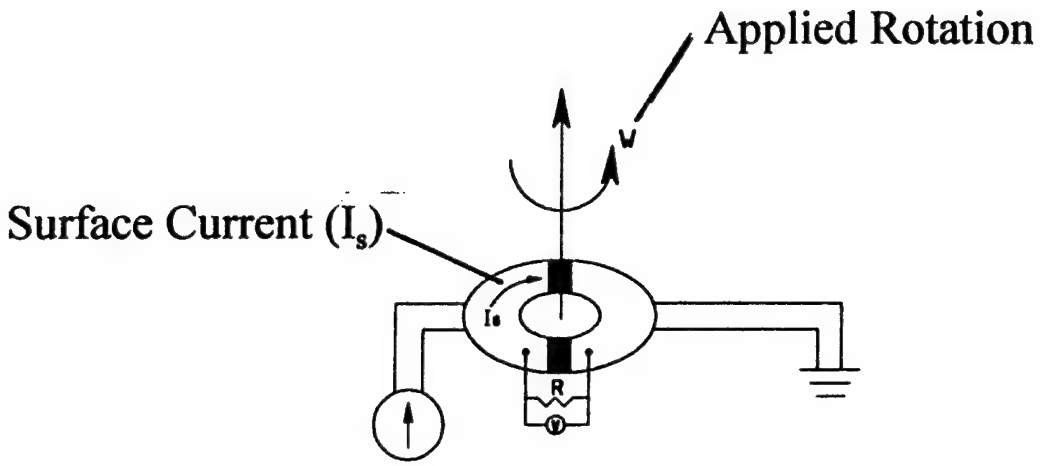

Figure 7 : Rotating SQUID

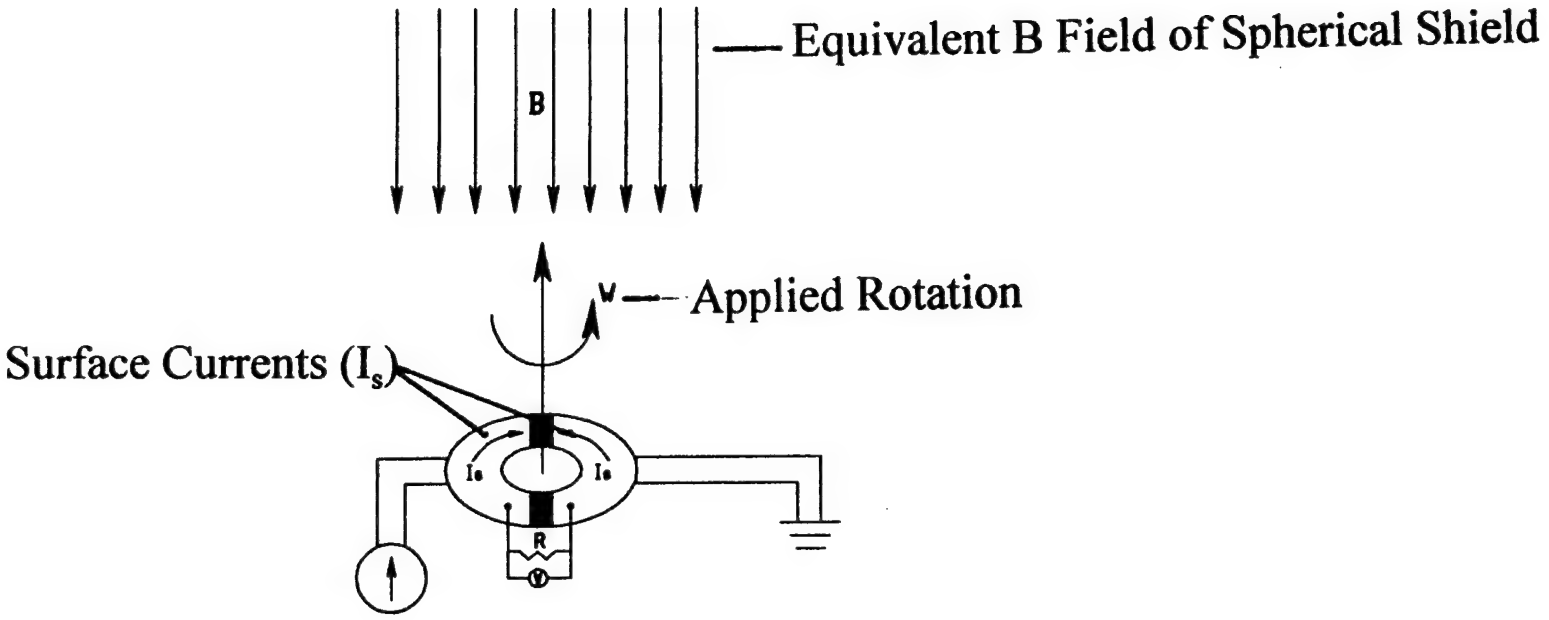

Figure 8 : Rotating SQUID in External Field

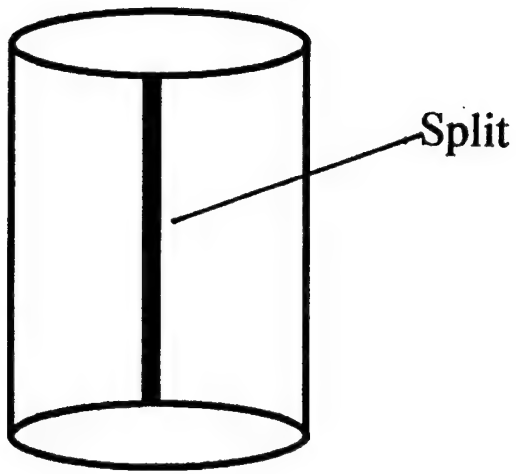

Figure 9 : Split Superconducting Magnetic Shield

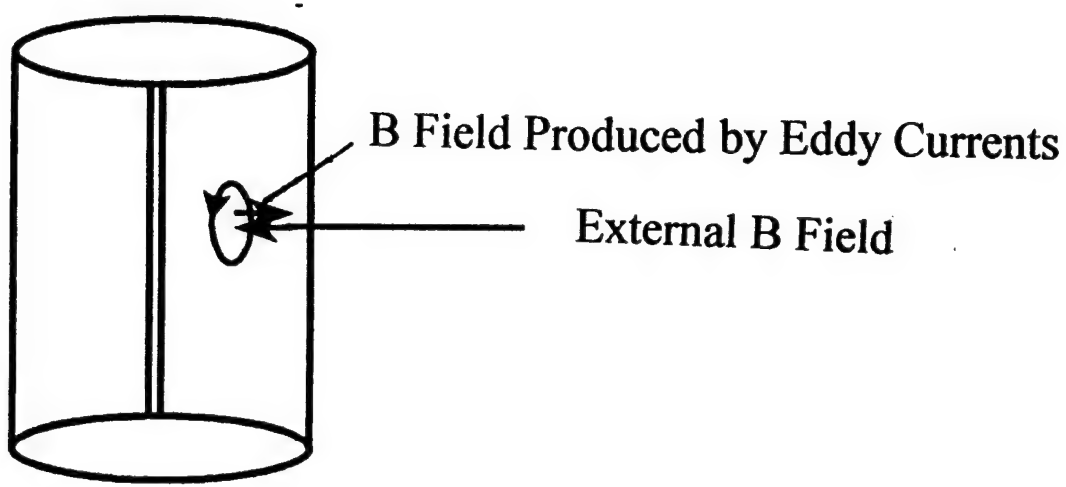

Figure 10 : Effect of Localized Eddy Currents Produced by External B Field

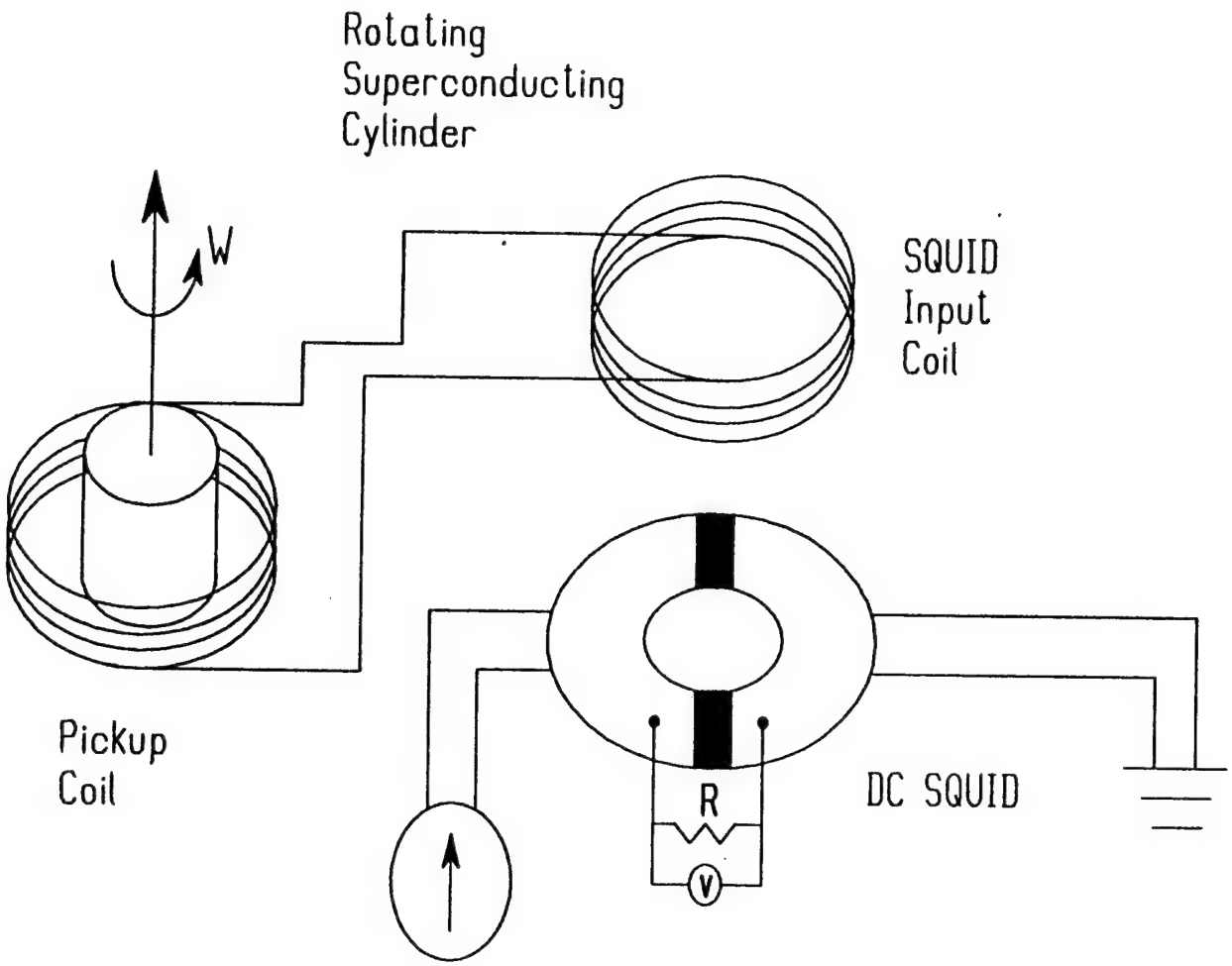

Figure 11 : SQUID with Pickup Circuit

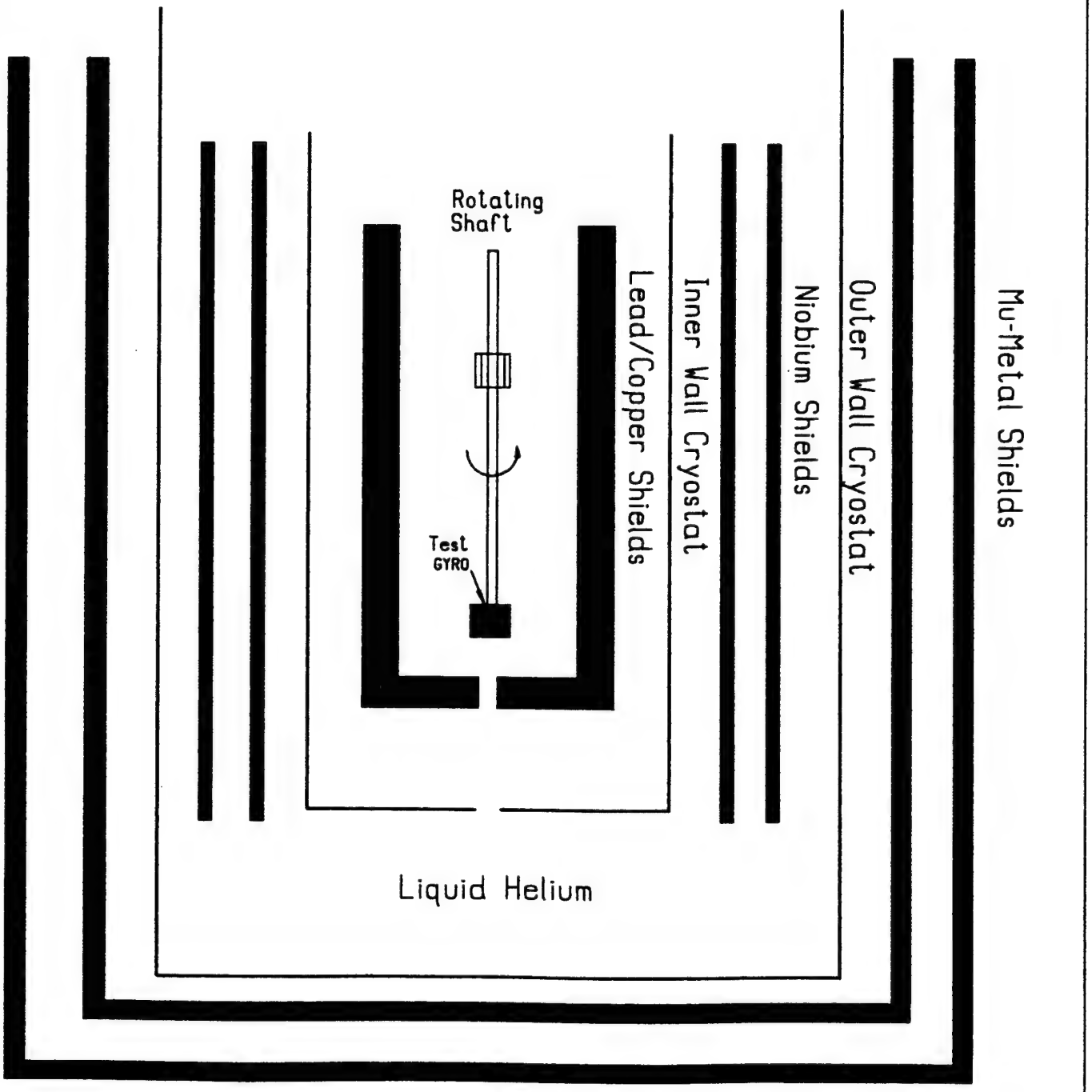

Figure 12 : Dewar with Nested Pb and Nb Magnetic Shields

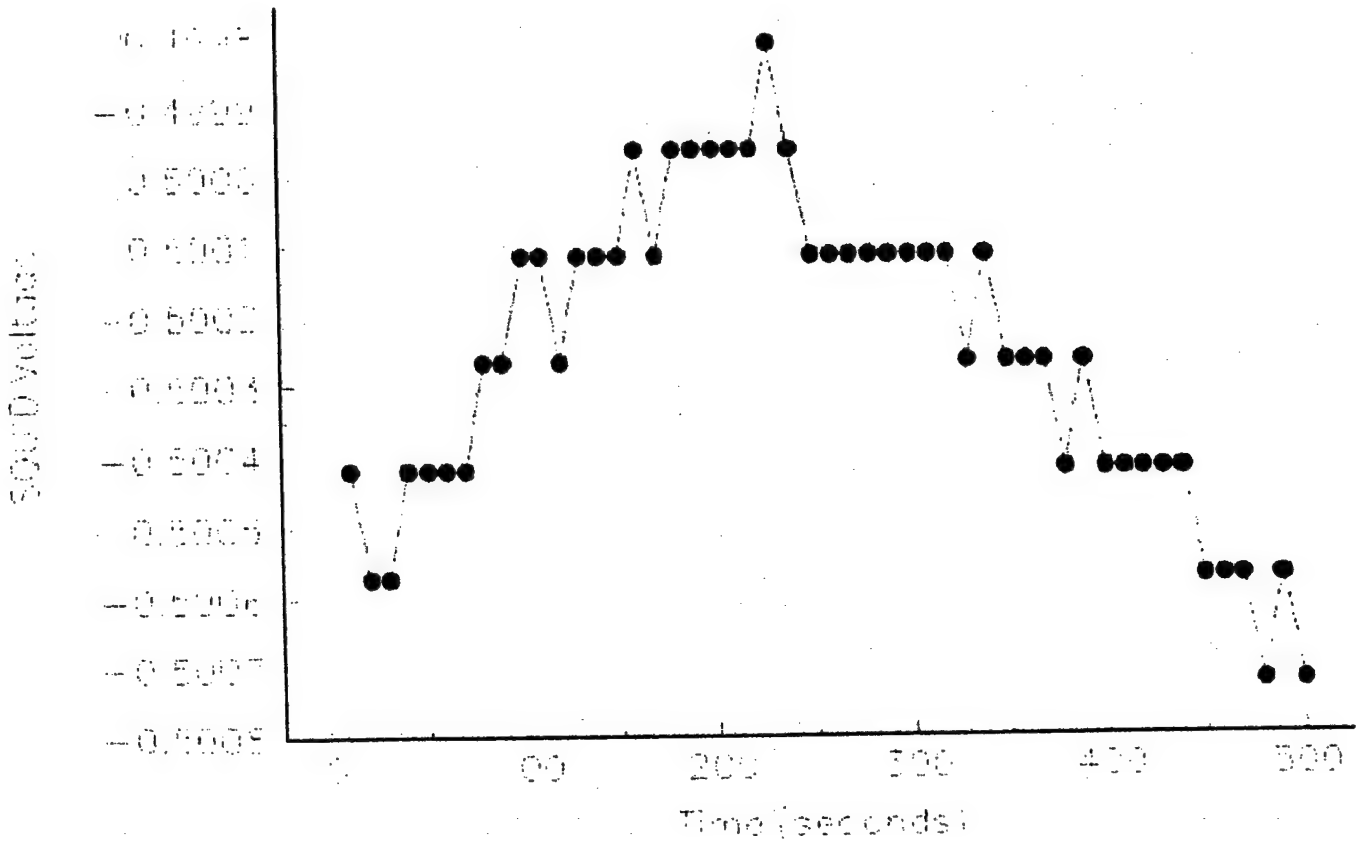

Figure 13: Work Area Magnetic Field vs Time

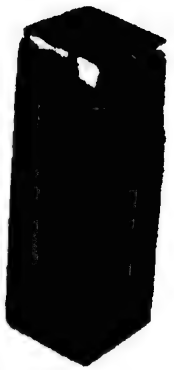

Figure 15: Parallelepiped SrTiO3 Crystal Coated with YBCO

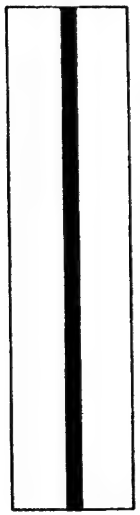

Figure 16: Scored Parallelpipe Head Crystal

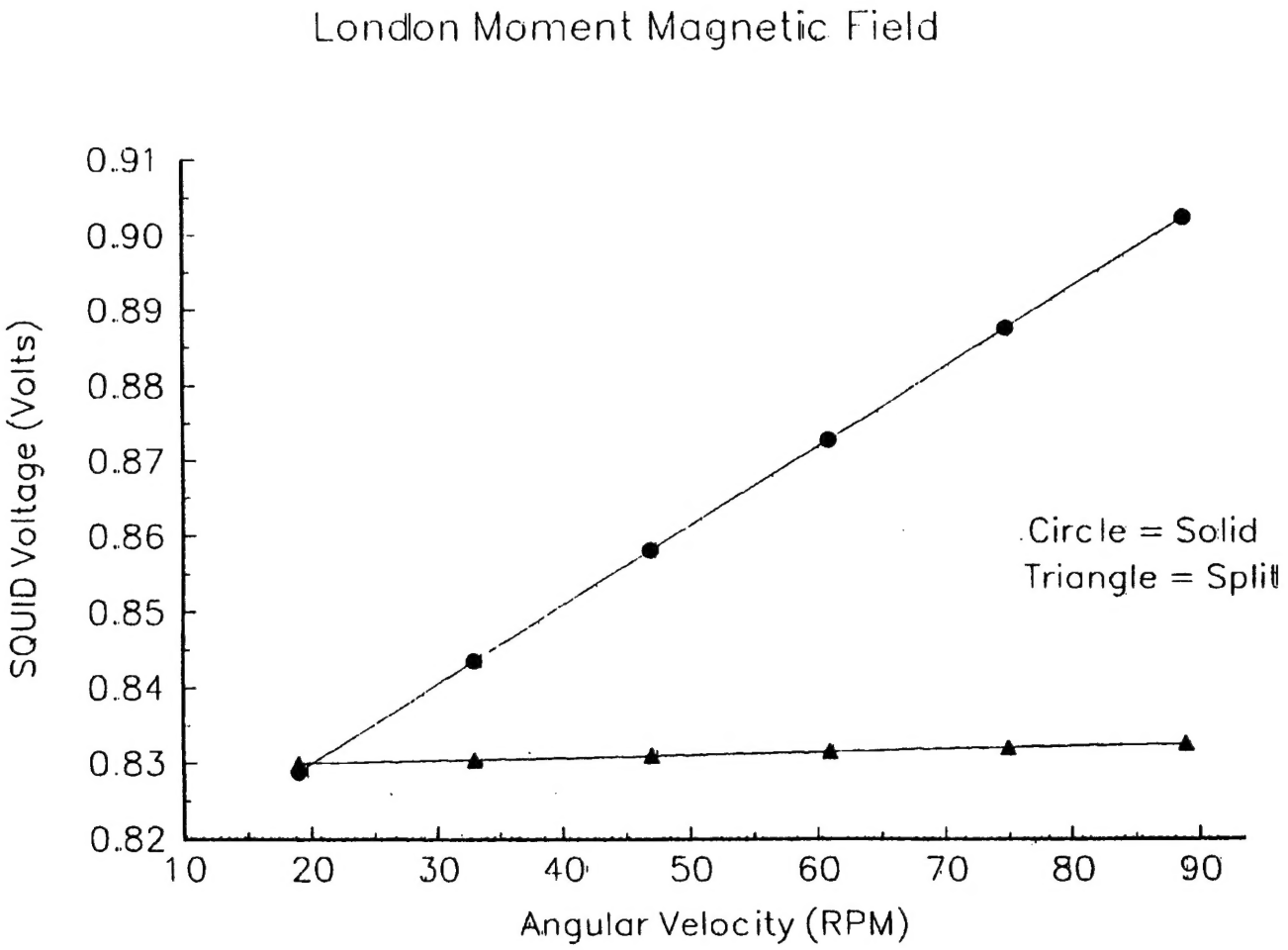

Figure 17: SQUID Voltage vs Angular Velocity for Solid and Split Shield

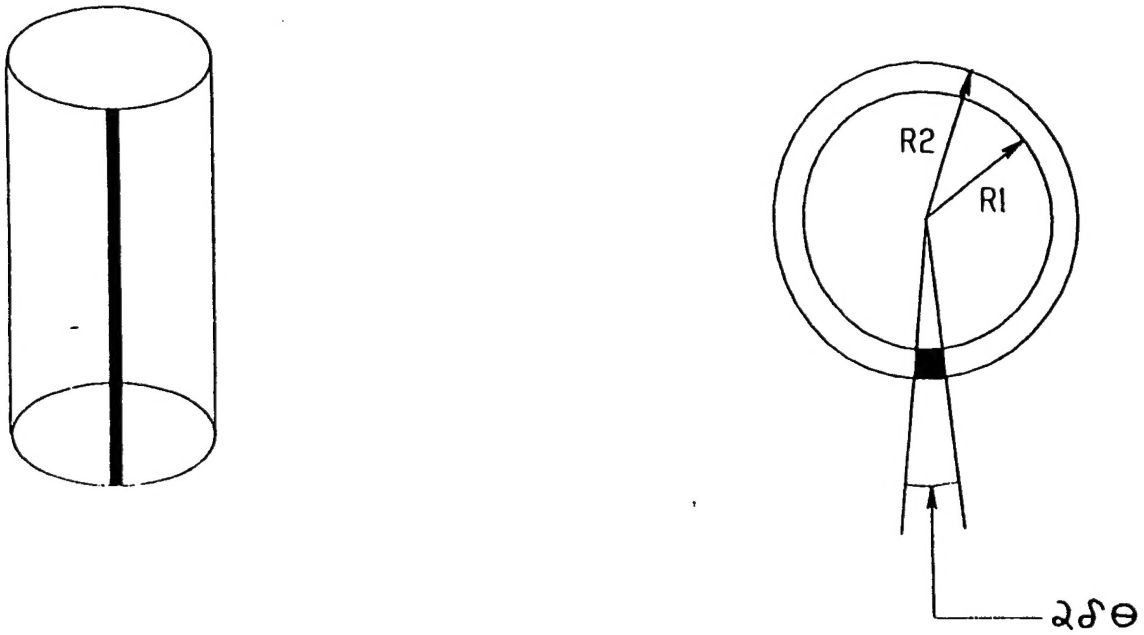

Figure 18: Split Superconducting Magnetic Shield

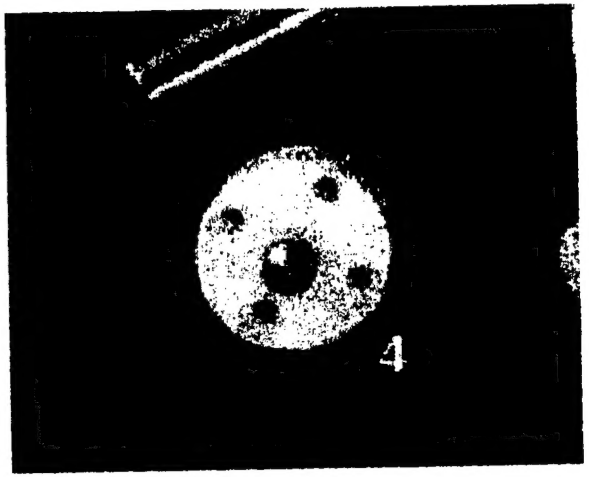

Figure 19: HfV2 Sample

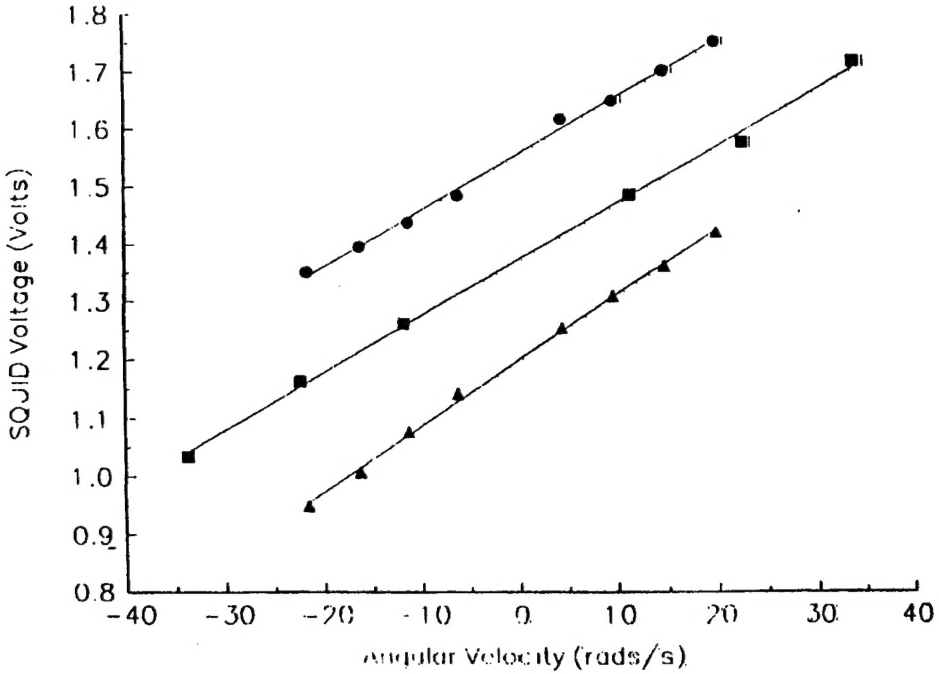

Figure 20 London Field Slope of Pb, BPSCCO and HfV2